Characterization of Coherent Structures from Parallel, LES Computations of Wandering Effects in Bubble Plumes

Fabián A. Bombardelli
Research Assistant, V. T. Chow Hydrosystems Laboratory, Dept. of Civil and Environmental Eng., University of Illinois at Urbana-Champaign, 205 North Mathews Ave., Urbana, IL 61801

Abstract

This paper is aimed at characterizing turbulence in bubble plumes undergoing a transient motion, a topic of primary importance in many environmental applications.

Mathematical models for dilute mixtures, derived from the two-fluid model equations (multiphase flow theory), are initially presented. These models include diverse degrees of complexity, and handle turbulence via a k-ε model and a Large-Eddy Simulation (LES) approach, in a consistent way. The models, implemented in a parallel code, are then used to numerically simulate the dynamic behavior of bubble columns in three dimensions, using the LES approach. The results of high-resolution simulations show the presence of coherent structures whose distributions in space, and number, change with time. These structures are characterized in the paper via several indicators, connecting them with potential events of breakup of bubbles.

Introduction

Bubbly flows are encountered in many fields of engineering, associated with different spatial scales. At the small scale, they are found for instance in metallurgy in gas stirring of ladles, in nuclear devices, and in chemical reactors. At extremely large scale, they take place in induced events of CO_2 sequestration, by which this compound is "injected" into deep seas. At the environmental scale, the application range is vast: bubble plumes have been used as barriers to contain density intrusions or oil spills, as breakwaters, as silt curtains, and in lakes for destratification purposes. In sanitary engineering, bubble plumes are usually employed for aeration purposes in water and wastewater treatment plants. Additionally, arrays of bubble diffusers are used in reservoirs aimed at storing combined sewer overflows, in order to avoid the occurrence of anaerobic conditions. This gives motivation for new experimental and numerical studies about bubble plumes.

Bubble plumes in vessels present a particular feature, which is the "wandering" phenomenon. In general, simple terms, the flow swarms from side to side within the container. No definite explanation for this behavior has been yet proposed, but there is certain evidence that it is produced via instabilities of the flow enhanced by the presence of walls (Pfleger et al., 1999).

Remarkable progress has been achieved in the last decade regarding modeling of gas-liquid flows. Still, there is no consensus about the best way to represent the "turbulence modulation or modification" of the carrier fluid induced by the disperse phase. This is intimately related to the turbulent dispersion of the latter produced by the carrier. The distribution of turbulence has consequences on the details of the non-linear processes of breakup and coalescence of bubbles.

This paper presents numerical simulations of the dynamic phenomenon of wandering in a bubble column, represented using an extremely dense mesh. Turbulence is accounted for through the use of a Large-Eddy Simulation (LES) approach. To the author's knowledge, only Deen et al. (2001) presented

dynamic simulations of *bubble columns using LES*, in an attempt to reproduce their own measurements, using a commercial code. The code used in the present paper, on the contrary, is an open-source code, and it has been run for longer times. Numerous turbulent scales appear in the numerical results, which are interpreted as a function of the dynamics of the phenomenon.

Review of the Experimental Tests Selected

The tests simulated herein are those of Becker et al. (1994). The experimental facility consisted of a flat apparatus with rectangular cross section. The cross section had 0.5 m of width and 0.08 m of thickness, while the main results were reported for a water depth of 1.5 m. Gas was input through a frit sparger located 10 cm to the left from the column center, at a rate of 1.6 l/min (other airflow rates were also tested). Liquid velocities were measured with a Laser Doppler Anemometer (LDA) and a microturbine anemometer. Bubble sizes and gas hold-up were also determined. Becker et al. (1994) presented their results in terms of distributions of gas and liquid velocities. These fields clearly revealed a transient, oscillating pattern, of quasi-periodic nature. Several circulation cells appeared in the flow field, changing in shape and number as time progressed in the quasi-period. Figure 1 depicts the temporal evolution of a surrogate of the air concentration, obtained through inverted photographs from the front face. Pictures were taken 5 seconds apart.

Theoretical Model

Hydrodynamic sub-models for the water and air phases depart from the two-fluid model (multiphase flow theory), obtained via ensemble averaging of the exact conservation equations for each phase in a multiphase flow. According to Drew and Passman (1999), this model reads:

- Conservation of mass for each fluid:

$$\frac{\partial \left(\alpha_k \left\langle \rho_k \right\rangle\right)}{\partial t} + \nabla \cdot \left(\alpha_k \left\langle \rho_k \right\rangle \left\langle \vec{v}_k \right\rangle\right) = \Gamma_k \tag{1}$$

- Conservation of momentum for each fluid:

$$\frac{\partial \left(\alpha_k \left\langle \rho_k \right\rangle \left\langle \vec{v}_k \right\rangle\right)}{\partial t} + \nabla \cdot \left(\alpha_k \left\langle \rho_k \right\rangle \left\langle \vec{v}_k \right\rangle \otimes \left\langle \vec{v}_k \right\rangle\right) + \alpha_k \nabla \left\langle p \right\rangle = \nabla \cdot \left\{\alpha_k \left[\left\langle \underline{\underline{T}}_k \right\rangle + \left\langle \underline{\underline{T}}_k^{\mathrm{Re}} \right\rangle\right]\right\} +$$
$$+ \alpha_k \left\langle \rho_k \right\rangle \left\langle \vec{b}_k \right\rangle + \vec{M}_k \tag{2}$$

where the subscript k stands for g in the case of the gaseous phase and for l in the liquid counterpart, $\langle \cdot \rangle$ denotes ensemble averaging operator, α_k is the volume fraction of fluid k, ρ_k is the density of fluid k, $\vec{v}_k$ is the velocity vector of fluid k, t is the time coordinate, and Γ_k is the mass transfer to phase k. Additionally, $\left\langle \underline{\underline{T}}_k \right\rangle$ refers to the "laminar" shear stress tensor, the shear stress tensor with the superscript "Re" is the result of the process of ensemble averaging, p is the pressure, assumed to be the same for the two fluids, $\vec{b}_k$ is the vector coming from body forces, and $\vec{M}_k$ indicates the interfacial forces exerted on fluid k. The sum of both aforementioned shear stress tensors is denoted simply by $\left\langle \underline{\underline{T}}_k^* \right\rangle$. In (2), a term accounting for the momentum transfer arising from mass transfer between phases has been neglected. Instead of solving the system involved in (1) and (2) in a strict way, *the liquid equations are*

replaced by equations for the mixture, obtained by addition of the mass and momentum equations for the liquid and the gas, using the following definitions:

$$\rho_m = \alpha_l \left\langle \rho_l \right\rangle + \alpha_g \left\langle \rho_g \right\rangle \qquad (3); \qquad \rho_m \ \vec{v}_m = \alpha_l \left\langle \rho_l \right\rangle \left\langle \vec{v}_l \right\rangle + \alpha_g \left\langle \rho_g \right\rangle \left\langle \vec{v}_g \right\rangle \qquad (4)$$

$$\underline{\underline{T_m}} = \alpha_l \left\langle \underline{\underline{T_l^*}} \right\rangle + \alpha_g \left\langle \underline{\underline{T_g^*}} \right\rangle \qquad (5); \qquad p_m = \left\langle p \right\rangle \qquad (6)$$

For a *dilute* bubble plume, this procedure gives rigorously (Buscaglia et al., 2002):

- Conservation of mass for the mixture:

$$\frac{\partial \left(\rho_m\right)}{\partial t} + \nabla \cdot \left(\rho_m \ \vec{v}_m\right) = 0 \qquad (7)$$

- Conservation of momentum for the mixture:

$$\frac{\partial \left(\vec{v}_m \ \rho_m\right)}{\partial t} + \nabla \cdot \left(\rho_m \ \vec{v}_m \otimes \vec{v}_m\right) + \nabla \, p_m = \nabla \cdot \underline{\underline{T_m}} + \ \rho_m \ \vec{g} \qquad (8)$$

where $\vec{g}$ indicates the vector related to the acceleration of gravity. The simulation of turbulence effects involves a second averaging (or filtering) process. This motivates that the stress tensor $\underline{\underline{T_m}}$ is approximated by the Reynolds stress tensor when using the k-ε model in a Reynolds-Averaged Navier-Stokes (RANS) equations environment, and it is given by the subgrid stress tensor in a LES approach.

Now, turning to the gaseous phase, it is assumed that only two gases compose the air, namely, oxygen and nitrogen. The above averaging issues apply for the gas mass equation as well. Using similar concepts to the above, the following mass conservation equations can be obtained (the equation pertaining to oxygen is provided; the one for nitrogen is analogous):

$$\frac{\partial \overline{\left\langle C_O \right\rangle}}{\partial t} + \nabla \cdot \left(\overline{\left\langle C_O \right\rangle} \ \overline{\left\langle \vec{v}_g \right\rangle} \right) = \overline{S_O} + \nabla \cdot \left[\frac{\mu_T}{\left\langle \rho_l \right\rangle Sc_g} \nabla \left(\overline{\left\langle C_O \right\rangle} \right) \right] \qquad (9)$$

where an isotropic version of the gas dispersion tensor has been adopted, C_O is the concentration of gaseous oxygen, in mol/m^3, S_O represents the source/sink term of oxygen, Sc_g is the Schmidt number, the operator $\overline{(\cdot)}$ indicates Reynolds averaging, and μ_T is the dynamic eddy viscosity. Next equation is used for the purpose of computing the gas density in terms of the gas concentrations:

$$\overline{\alpha_g \left\langle \rho_g \right\rangle} = \overline{\left\langle C_O \right\rangle} \, \mathrm{M}_O + \overline{\left\langle C_N \right\rangle} \, \mathrm{M}_N \approx \overline{\alpha_g} \left\langle \rho_g \right\rangle \qquad (10)$$

being M_i the molecular weight of gas i. Another closure relation is needed for the gas volume fraction, employing the well-known ideal gas law:

$$\overline{\alpha_g} = \frac{\left(\overline{\left\langle C_O \right\rangle} + \overline{\left\langle C_N \right\rangle} \right) R \, T_g}{\overline{\left\langle p_g \right\rangle}} \qquad (11)$$

where T_g, the gas temperature, is assumed as homogeneous and constant in time. An extra equation for the density of bubbles, N_b, is solved, as follows:

$$\frac{\partial \overline{N_b}}{\partial t} + \nabla \cdot \left(\overline{N_b} \ \overline{\left\langle \vec{v}_g \right\rangle} \right) = \nabla \cdot \left[\frac{\mu_T}{\left\langle \rho_l \right\rangle Sc_g} \nabla \left(\overline{N_b} \right) \right] \qquad (12)$$

The sources/sinks $\overline{S_O}$ and $\overline{S_N}$ represent the mass transfers from the gaseous to the dissolved phases. The concentrations of dissolved oxygen and nitrogen, C_{dO} and C_{dN}, can be modeled in a totally equivalent way as done with the gaseous phase, equation (9), using a Schmidt number for the liquid and employing

the liquid velocity instead of the gaseous one. The *mixture* velocity is used to approximate the *liquid* velocity in this model. For the source/sink terms, the standard linear expression is utilized. The equivalent bubble radius, r_b, can be computed from the bubble volume, in turn obtained with the help of:

$$\overline{v_b} = \frac{\left(\overline{\langle C_O \rangle} + \overline{\langle C_N \rangle}\right) R\, T_g}{\overline{\langle p_g \rangle}\ \overline{N_b}} \tag{13}$$

To solve (9), and (12), it is necessary to know the gas velocity. The computation can be achieved in many ways. One of them is solving the "full" gas momentum equation. To that end, the forces included in $\vec{M}_g$ in (2) need to be specified. Alternatively, an *algebraic* model for the gas can be used as follows:

$$\overline{\langle \vec{v}_g \rangle} = \overline{\langle \vec{v}_l \rangle} + w_b \vec{k} \tag{14}$$

The last vector indicates the slip velocity, which points in the vertical direction and whose magnitude is specified in terms of the equivalent bubble radius (see Wüest et al., 1992).

In the implementation used in this code, the velocity of the mixture and the relative velocity of the gas were selected as main degrees of freedom for velocity. This choice has been found more convenient than the usual one (namely the velocity of the liquid and the velocity of the gas), for a hierarchical organization of the models. Of course, given the mixture velocity and the relative velocity, one can compute the liquid and gas velocities if the gas fraction is known, so that the formulations are equivalent except for minor details. As variant of the model, it is possible to use the Boussinesq approximation for the mixture by which (7) and (8) yield equations with the shape of the Navier-Stokes equations. The code allows for the selection of different stabilization techniques of the finite element method, by which the equations have been solved.

One of the two ways of dealing with turbulence implemented in the code is the *standard* k-ε model. This model has been used in dynamic simulations *by Sokolichin and Eigenberger (1999), Borchers et al. (1999), Pfleger et al. (1999) and Buwa and Ranade (2002).* A treatment based on LES is also implemented, with the subgrid viscosity represented using the Smagorinsky's model, as follows:

$$\nu_{sgs}(\vec{x}, t) = (C_s\ \Delta)^2 \left(2\left|\hat{S}(\vec{x}, t)\right|^2\right)^{1/2} \tag{15}$$

where $\hat{S}(\vec{x}, t)$ indicates the characteristic filtered rate of strain tensor, and its magnitude refers to its double contracted product. C_s in turn is the Smagorinsky coefficient.

The parallel code runs in the IA-64 Linux Cluster of the National Center of Supercomputing Applications (NCSA) at Urbana-Champaign. Tetrahedral elements were used.

Simulation of Dynamic Conditions. Analysis of coherent structures and turbulence

The present simulations were obtained with the algebraic model, which is very similar to Sokolichin and Eigenberger's model (1999). Moreover, instead of computing the bubble-slip velocity in terms of the bubble radius, a constant value of 0.2 m/s (throughout the flow field) was specified, with the same approach of the above authors. The runs were performed first with the k-ε model (not shown herein) and, then, with the LES treatment. The algebraic model for the gas was kept the same with the k-ε model and the LES approach. For the LES runs, 2,870,400 elements were employed, corresponding to a spatial step of 0.005 m (5 mm) and to a mesh of 300 x 16 x 100. The spatial resolution in these runs is twice that of Deen et al.'s. Time step was 0.1 seconds, which is compatible with the spatial resolution

employed, according to the existing domain-averaged, convective velocities. No mass-transfer effects were included in these simulations. The runs with LES were highly demanding, requiring 7 hours per 9 seconds of simulation at the Linux Cluster with 20 processors. Runs were performed for 400 seconds of simulation time, which cover about 8 periods. Figure 2 shows snapshots of the gaseous oxygen concentration for the case of the LES simulation, demonstrating the unsteady behavior involved in the wandering phenomenon. They comprise a period of the dynamic motion, which was slightly larger than the measured one. The results are separated by 5.5 seconds. If the snapshots of Figure 2 are compared to those of Figure 1, a clear correspondence is observed. This means that the simulation mimics satisfactorily the measurements, which is also true for the $k-\varepsilon$ model simulations (not shown herein). Figure 3 presents the velocity fields pertaining to the above oxygen concentrations, expressed in velocity magnitude. Larger values of velocity magnitude are presented in yellow, being of the order of 0.5 m/s. Notice the large *coherent structures* present in the figure, *embedded in a wide spectrum of smaller scales*. These structures are almost coincident with those obtained by Sokolichin and Eigenberger (1999), via a $k-\varepsilon$ model, and also with those captured in $k-\varepsilon$-model runs done with the present code. However, the level of detail allowed by the LES solution is unique, and indeed contributes significantly to the understanding of the flow. The large motion scales are basically determined by the geometry of the problem, as expected, but the interaction with the plume wandering determines the specific number of vortices present at a given time. Notice that this number of vortices goes from 1 to 2, and then to 3, to finally undergo the inverse pathway, as reported by Sokolichin and Eigenberger (1999). The size of these vortices of horizontal axis is variable, but does not decrease from, say, 0.15 m (15 cm).

Numerous variables can be determined from the "instantaneous" velocity fields, in vertical planes parallel to the front face of the bubble column. Figure 4 addresses the following, from left to right: a) the magnitude of the velocity vectors at the central plane for one of the times (obtained only with the vertical and horizontal components), in m/s; b) the component of the vorticity vector perpendicular to the front face of the bubble column, in 1/s (values in figure are multiplied by 10^3); c) the gradient of the vertical velocity (W) with respect to the horizontal coordinate, in 1/s (values in figure are multiplied by 10^3). This situation pertains to the case of 3 vortices for a plane right in the middle of the thickness. Relatively small scales (of the order of 1 or 2 cm) are associated to the "pathways" of the bubbles, but they are present in several other places as well. Notice that these relatively small scales are larger than the Kolmogorov scale (of the order of 0.5 to 1.6 mm) and than the bubble size, which is of 3 mm. Zones of large velocity gradients are useful at the time of identifying regions in which bubbles are subjected to high shear and, thus, in which bubbles could experience events of breakup. These zones are located mainly in the borders of the large-scale vortices, as expected, which in turn encompass regions with and without bubbles.

Figure 5 depicts the same results but for a vertical plane located at 1 cm from the wall. In general terms, the same structures appear, suggesting a quasi-two-dimensional flow. However, notice that certain small and intermediate scales present in the central plane (Figure 4) are smoothed in the plane close to the wall (Figure 5).

Conclusions

A simulation using the LES approach with Smagorinsky's model has been presented. The results have been found to agree well with the experiments. This is not a trivial result considering that finite elements of moderate order (with linear interpolation) have been employed. These simulations are highly intense, since a very dense mesh has been used. The results show the capabilities of multiphase flow theory, together with computational fluid dynamics (CFD), to study environmental problems. It is confirmed

that *algebraic* models (usually regarded as simple, approximate models) are capable of capturing the quasi-periodic wandering motion of the bubbles in 3D simulations. In these experiments, the main forces are drag and buoyancy and no additional force is needed to obtain wandering (additional forces were included by Mudde and Simonin, 1999), either with the $k-\varepsilon$ model (not shown herein) or with LES. This result is important regarding the good agreement with measurements obtained in these simulations using both approaches.

A qualitative as well as a quantitative characterization of the coherent structures within the bubble column has been undertaken and presented. Zones of high velocity gradients have been identified and have been found to present a quasi-two-dimensional behavior. However, relatively small and intermediate scales are affected close to the wall.

Finally, the present results are thought to be useful in two ways. First, in underscoring the science of the wandering phenomenon; second, in gaining understanding conducive to the design of arrays of bubble plumes in different applications, in which wandering effects are relevant, and where the effects of the presence of walls are important.

Acknowledgements

The account at the NCSA awarded to Prof. Marcelo H. García is gratefully acknowledged. This research was funded by the US Army Corps of Engineers, under Research Contract DACW42-00-P-0396. This support is gratefully acknowledged.

References

Becker, S., Sokolichin, A., and Eigenberger, G. (1994). "Gas-liquid flow in bubble columns and loop reactors: part II. Comparison of detailed experiments and flow simulations." *Chem. Eng. Sci.*, 49(24B), 5747-5762.

Borchers, O., Busch, C., Sokolichin, A., and Eigenberger, G. (1999). "Applicability of the standard k-ε turbulence model to the dynamic simulation of bubble columns. Part II." *Chem. Eng. Sci.*, 54, 5927-5935.

Buscaglia, G. C., Bombardelli, F. A., and García, M. H. (2002). "Numerical modeling of large-scale bubble plumes accounting for mass transfer effects." *Int. J. Multiphase Flow*, 28, 1763-1785.

Buwa, V. V., and Ranade, V. V. (2002). "Dynamics of gas-liquid flow in a rectangular bubble column: experiments and single/multi-group CFD simulations." *Chem. Eng. Sci.*, 57, 4715-4736.

Deen, N. G., Solberg, T., and Hjertager, B. H. (2001). "Large eddy simulation of the gas-liquid flow in a square cross-sectioned bubble column." *Chem. Eng. Sci.*, 56, 6341-6349.

Drew, D. A., and Passman, S. L. (1999). "*Theory of multicomponent fluids."* Spinger-Verlag, N. Y..

Mudde, R. F., and Simonin, O. (1999). "Two- and three-dimensional simulations of a bubble plume using a two-fluid model." *Chem. Eng. Sci.*, 54, 5061-5069.

Pfleger, D., Gomes, S., Gilbert, N., and Wagner, H.-G. (1999). "Hydrodynamic simulations of laboratory scale bubble columns fundamental studies of the Eulerian-Eulerian modelling approach." *Chem. Eng. Sci.*, 54, 5091-5099.

Sokolichin, A., and Eigenberger, G. (1999). "Applicability of the standard $k-\varepsilon$ turbulence model to the dynamic simulation of bubble columns: Part I. Detailed numerical simulations." *Chem. Eng. Sci.*, 54, 2273-2284.

Wüest, A., Brooks, N. H., and Imboden, D. M. (1992). "Bubble plume modeling for lake restoration." *Water Resources Research*, 28(12), 3235-3250.

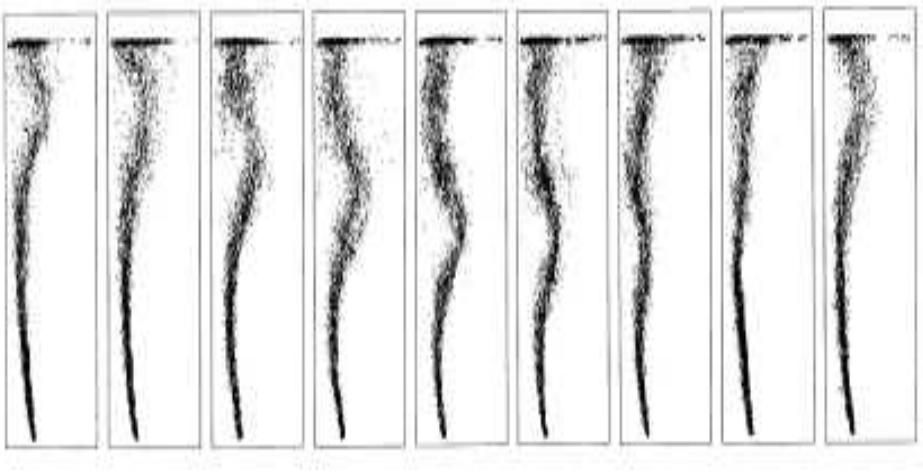

Figure 1: Motion of bubbles in a bubble column (from Sokolichin and Eigenberger, 1999). The sequence was obtained using inverted photographs. The bubble column has 0.08 m in the direction perpendicular to the paper

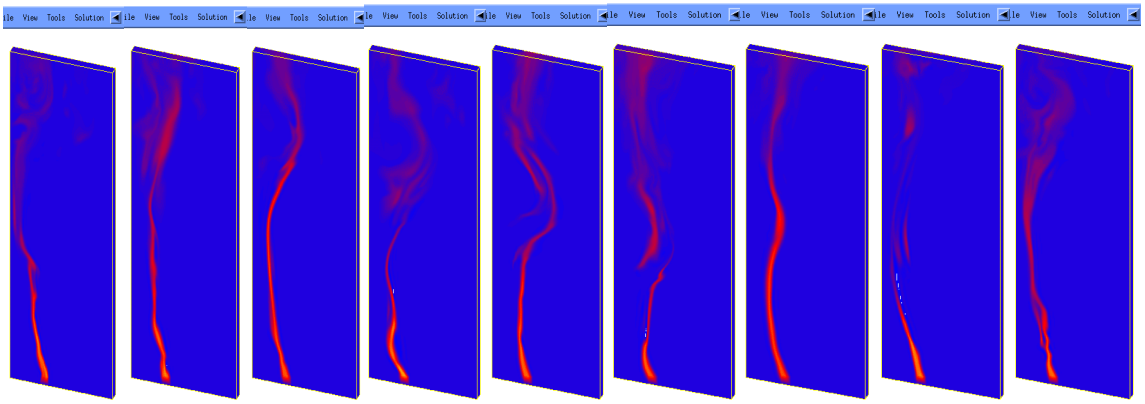

Figure 2: Snapshots of gaseous oxygen concentration for the dynamic simulation, using a LES approach

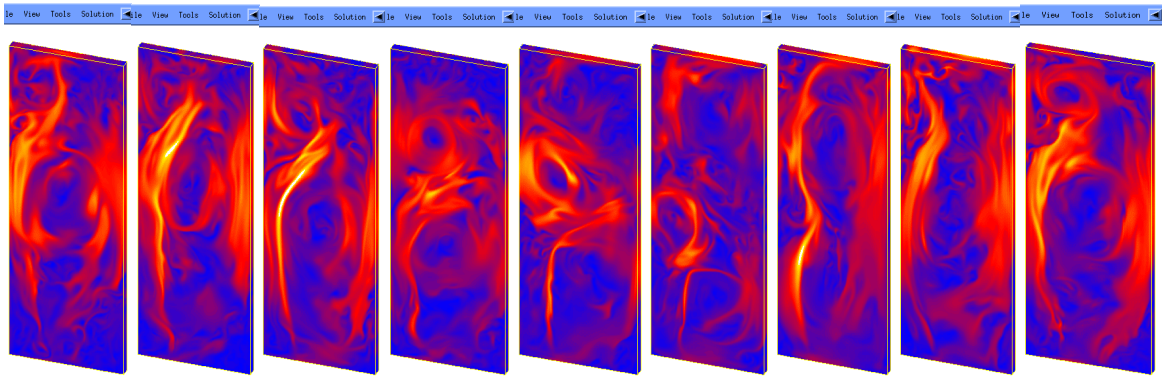

Figure 3: Snapshots of velocity magnitude for the dynamic simulation, using a LES approach

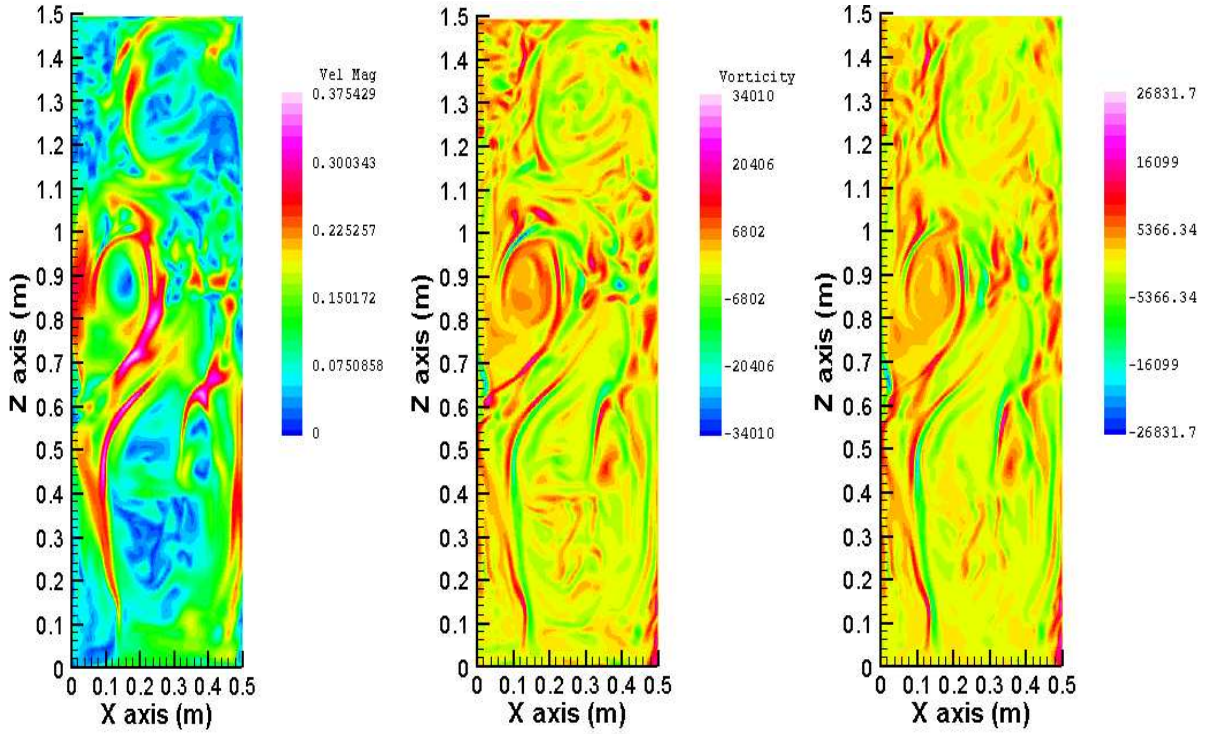

Figure 4: Snapshots of velocity magnitude, vorticity and dW/dx, from LES approach. Plane corresponding to the center position in the thickness. Values of vorticity and dW/dx are multiplied by 10^3.

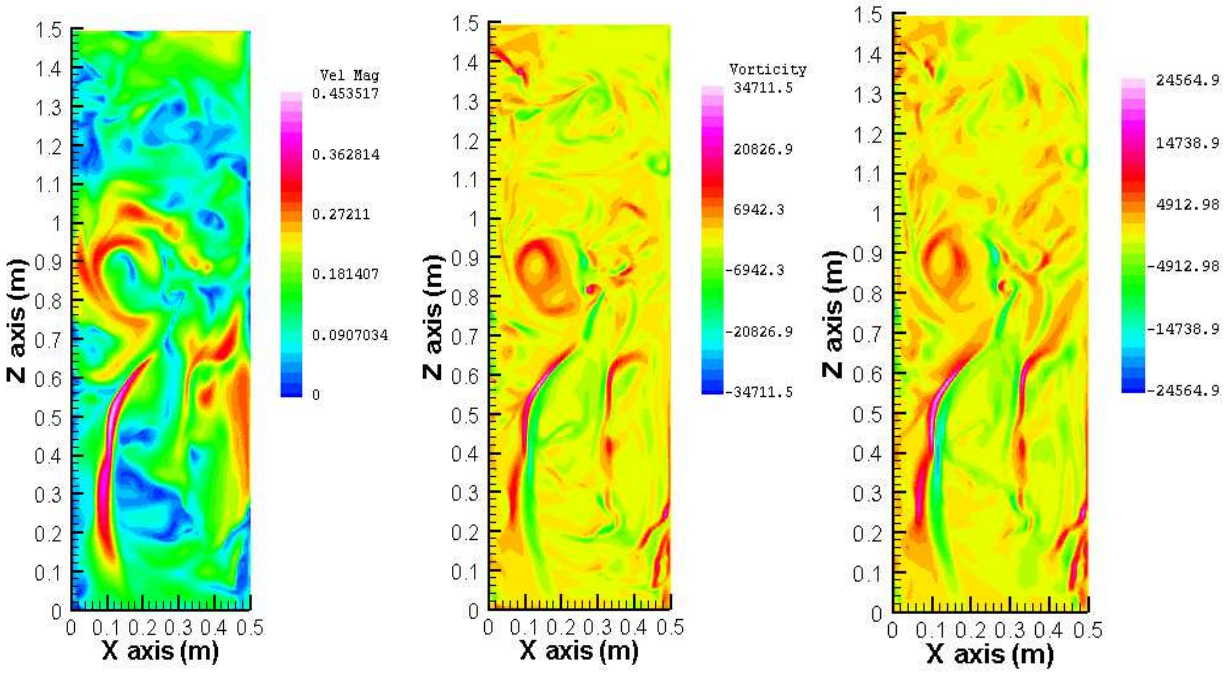

Figure 5: Snapshots of velocity magnitude, vorticity and dW/dx, from LES approach. Plane corresponding to 1 cm from the front wall in the thickness. Values of vorticity and dW/dx are multiplied by 10^3.